THE PERSISTENCE OF HIGH ALTITUDE NON-EQUILIBRIUM DIFFUSE IONIZED GAS IN SIMULATIONS OF STAR FORMING GALAXIES

СОХРАНЕНИЕ СО ВРЕМЕНЕМ НЕРАВНОВЕСНОГО DIG НА БОЛЬШИХ ВЫСОТАХ В СИМУЛЯЦИЯХ ЗВЕЗДООБРАЗУЮЩИХ ГАЛАКТИК

https://academic.oup.com/mnras/article/530/3/2548/7643656

arXiv:2404.05651

Постникова Вера (ФФ МГУ, ГАИШ МГУ)

VoLGa, 19 июня 2024 г.

Напоминание о свойствах DIG для MW

The Galactic DIG is inferred to have an average electron density of 0.01–0.1 cm^{-3}, with a scale height of approximately 1 kpc (Haffner et al. (2009)). Scale heights of H α emission (roughly half the electron density scale height) throughout the Milky Way have been measured in the range 250 pc to greater than 1 kpc (Hill et al. 2014; Krishnarao et al. 2017). Ocker, Cordes & Chatterjee (2020) measure the free electron scale height in the local Galactic disc to be approximately 1.5 kpc via pulsar dispersion measures. The temperature of the DIG is higher than that of typical H II regions, at 6000 to 10 000 K (Madsen, Reynolds & Haffner 2006). The DIG requires both

- Электронная плотность 0.01–0.1 $см^{-3}$
- Температура 6000 К – 10 000 К (выше, чем в областях H II)
- Средняя шкала высот плотности электронов — порядка 1 кпк
- Локальная шкала высот свободных электронов — порядка 1.5 кпк
- Шкала эмиссии Ha — от 250 пк до более чем 1 кпк

Проблемы DIG - 1

K (Madsen, Reynolds & Haffner 2006). The DIG requires both a mechanism for supporting the ionized gas at high altitudes and also for providing the energy to ionize the gas. Many groups have

Vandenbroucke & Wood (2019) investigated the effect of photoionization on the support of DIG in simulations excluding supernovae. They found that outflows produced by the warm ionized gas were not enough to produce a DIG layer at the observed densities.

Cox 1993; Dove & Shull 1994). Until recently, the inclusion of photoionization in the large-scale feedback simulations was mostly done as a post-processing step on snapshots of the density grids and adopting ionization equilibrium. Compared to a smooth ISM,

Kado-Fong et al. (2020) performed MHD simulations of the ISM including the effects of supernovae, using a self-consistent star formation algorithm based on sink particle formation and the assumption of ionization equilibrium. The vertically resolved neutral structure reproduced that of the Milky Way, but the DIG layer in their simulations was highly variable in time and only occasionally reached the kpc scale heights inferred from observations. The assumption of ionization equilibrium and the absence of accreting gas from the intergalactic medium were suggested as possible explanations for the low density of the DIG in their simulations. Another source of ionization of the DIG in addi-

- Механизмы для вброса и поддержания присутствия газа на больших высотах — ? (см. также следующий слайд)
- Механизмы, способные обеспечить наблюдаемую степень ионизации — ?
- Корректное моделирование, а именно:
  - — необходимость учитывать фидбек от сверхновых (Vandenbroucke & Wood 2019) — ?
  - — некорректность допущения ионизационного равновесия и расчета фотоионизационных эффектов на стадии пост-обработки моделей (Kago-Fong et al. 2020) — ?

Проблемы DIG – 2

simulations. Another source of ionization of the DIG in addition to OB stars is photoionization from a population of hot low mass evolved stars (often referred to as HOLMES). These sources have much lower ionizing luminosities than OB stars, but exist in greater numbers and at higher altitudes above the midplane (e.g. Byler et al. 2019). Rand et al. (2011), Flores-Fajardo et al. (2011), and Vandenbroucke & Wood (2019) showed that some of the trends of emission lines observed in the DIG can be partially explained by the combination of ionizing photons from OB stars plus a more vertically extended population of hot evolved low mass stars. The ionizing luminosities and spectra of these evolved low mass stars are uncertain for the Milky Way; characterization of these populations with *Gaia* may provide improved constraints on their contribution to the total ionizing luminosity.

- Необходимость учитывать HOLMES (hot low mass evolved stars), помимо OB-звезд — ?
    - HOLMES обладают меньшими ионизирующими светимостями, чем OB-звезды, но их число намного больше, тем более на больших высотах над плоскостью (т.к. OB-звезды сосредоточены в диске, а HOLMES распределены более равномерно по толстому диску и звездному гало)

Что из себя представляет данная работа?

Our work presented in this paper will focus firstly on the investigation of the two mechanisms required to generate a DIG layer, specifically whether the combined effects of feedback from supernovae and ionizing photons can elevate and maintain the ionization state of gas high above the mid-plane. Simulations implementing a time-dependent ionization calculation will be compared to those assuming ionization equilibrium. We will also investigate the effect on the density and scale height of the DIG from a component of hot evolved low mass stars contributing to the ionizing photon budget. The work presented here is an extension of Vandenbroucke & Wood (2019) to include supernovae feedback along with improvements in the simulation of star formation, photo- and collisional ionization mechanisms, and time-dependent ionization and recombination.

- Продолжение и расширение работы Vandenbroucke & Wood (2019) с учетом фидбека от суперновых + другие улучшения моделирования
- Фокус на исследовании двух механизмов для генерации слоя DIG (OB-звезды + HOLMES) + учет влияния фидбека от сверхновых на распространение фотонов + расчет моделей с учетом временных факторов и отсутствия ионизационного равновесия
    - Может ли это обеспечить существование и сохранение DIG на больших высотах с наблюдаемой степенью ионизации — ?

Сохранение (со временем) неравновесного DIG на больших галактических высотах в симуляциях звездообразующих галактик (по типу MW)

Monthly Notices of the ROYAL ASTRONOMICAL SOCIETY

MNRAS **530,** 2548–2564 (2024) https://doi.org/10.1093/mnras/stae988
Advance Access publication 2024 April 10

The persistence of high altitude non-equilibrium diffuse ionized gas in simulations of star-forming galaxies

Lewis McCallum,[1]★ Kenneth Wood,[1] Robert Benjamin,[2] Camilo Peñaloza,[1] Dhanesh Krishnarao,[3] Rowan Smith [1] and Bert Vandenbroucke [4]

[1] *School of Physics and Astronomy, University of St Andrews, North Haugh, St Andrews KY16 9SS, UK*
[2] *Department of Physics, University of Wisconsin-Whitewater, Whitewater, WI 53190, USA*
[3] *Department of Physics, Colorado College, Colorado Springs, CO 80903, USA*
[4] *Leiden Observatory, Leiden University, PO Box 9513, 2300 RA Leiden, the Netherlands*

Accepted 2024 April 8. Received 2024 March 15; in original form 2023 November 17

ABSTRACT

Widespread, high altitude, diffuse ionized gas with scale heights of around a kiloparsec is observed in the Milky Way and other star-forming galaxies. Numerical radiation-magnetohydrodynamic simulations of a supernova-driven turbulent interstellar medium show that gas can be driven to high altitudes above the galactic mid-plane, but the degree of ionization is often less than inferred from observations. For computational expediency, ionizing radiation from massive stars is often included as a post-processing step assuming ionization equilibrium. We extend our simulations of an Milky Way-like interstellar medium to include the combined effect of supernovae and photoionization feedback from mid-plane OB stars and a population of hot evolved low mass stars. The diffuse ionized gas has densities below 0.1 cm^{-3}, so recombination time-scales can exceed millions of years. Our simulations now follow the time-dependent ionization and recombination of low density gas. The long recombination time-scales result in diffuse ionized gas that persists at large altitudes long after the deaths of massive stars that produce the vast majority of the ionized gas. The diffuse ionized gas does not exhibit the large variability inherent in simulations that adopt ionization equilibrium. The vertical distribution of neutral and ionized gas is close to what is observed in the Milky Way. The volume filling factor of ionized gas increases with altitude resulting in the scale height of free electrons being larger than that inferred from H α emission, thus reconciling the observations of ionized gas made in H α and from pulsar dispersion measurements.

Key words: methods: numerical – H II regions – ISM: structure – ISM: kinematics and dynamics – galaxies: ISM – galaxies: star formation.

- Обычно симуляции турбулентной (из-за сверхновых) ISM показывают, что газ может быть закинут на большие галактические высоты, но степень его **ионизации** оказывается ниже, чем предполагается из наблюдений
- В таких моделях ионизирующее излучение подключается на этапе пост-обработки, при этом предполагается **ионизационное** равновесие
- Авторы симулируют MW-like ISM и включают в симуляцию фидбек от сверхновых и фотоионизацию от OB-звезд и HOLMES с учетом временных факторов при отсутствии ионизационного равновесия
- Большое время рекомбинации (~ и > миллионов лет) среды с плотностью 0.1 $см^{-3}$ и ниже позволяет DIG на больших высотах сохраняться еще долго после смерти массивных звезд
- В результате симуляций авторов вертикальное распределение нейтрального и ионизованного газа получается близким к наблюдаемому в MW

Методы - 1

5 CONCLUSIONS

In this work, we have further developed the simulations of Vandenbroucke & Wood (2019) to model the diffuse ionized gas in star-forming regions of spiral galaxies. We have modified the simulations to track explicit photoionization heating terms and cooling rates from De Rijcke et al. (2013). This allowed us to implement supernovae feedback in the form of thermal and kinetic energy injection. To ensure the accuracy of the ionization balance calculation at high temperatures (now present due to supernova feedback), thermal collisional ionization of the gas was implemented to complement the existing photoionization schemes. A more complex and self-consistent algorithm for star formation was implemented, including an SFR variation with mid-plane density, and the ability to generate source positions within the densest regions of the mid-plane. A background type Ia supernova rate was also implemented.

- Продолжили развивать подход Vandenbroucke & Wood (2019) **для DIG в звездообразующих областях** спиральных галактик
- Модифицировали симуляции для фотоионизационного нагрева и скорости охлаждения по данным De Rijcke et al. (2013)
- Учли фидбек от сверхновых в форме вброса тепловой и кинетической энергии
- Помимо фотоионизации учли тепловую столкновительную ионизацию газа для точного расчета ионизационного баланса при высоких температурах (из-за фидбека от сверхновых)
- Реализовали более сложный и самосогласованный алгоритм для звездообразования, учитывающий изменение SFR в зависимости от плотности в плоскости диска, а также позволяющий генерировать положения источников в наиболее плотных областях средней плоскости
- Реализовали взрывы сверхновых типа Ia в фоновом режиме (так как это не следовало автоматически из заданной симуляции)

Методы - 2

- Эмиссионные линии элементов, кроме водорода: He, C, N, O, Ne, and S, — не рассматривались (но обещают в будущем учесть и другие элементы)

Методы - 3

Схема моделирования

2.1 Radiation-hydrodynamics simulations

The results presented in this paper are from simulations using the Monte Carlo radiation-hydrodynamics code `CMacIonize` (Vandenbroucke & Wood 2018; Vandenbroucke & Camps 2020) in task-based mode. Starting from initial conditions described below, we run all simulations to a time of 300 Myr, with the fiducial simulation being run to 500 Myr.

2.1.1 Grid properties

2.1.2 Equation of state

2.1.3 Photoionization feedback

2.1.4 Time-dependent ionization calculation

2.1.5 Supernova feedback

2.1.6 Star formation

2.1.7 Hot low mass evolved stars

2.2 Initial conditions

2.2.1 Density and temperature structure

2.2.2 External potential

Результаты - 1

Table 1. Table of main simulation parameters and resulting vertical structures of ionized hydrogen. DIG is defined as ionized gas with $300K < T < 15000K$.

Model name	меняется со временем SFR ($M_\odot yr^{-1}kpc^{-2}$)	HOLMES luminosity ($s^{-1}HOLMES^{-1}$)	Escape fraction	Ion state limiter	Resolution (pc)	DIG n_0 (cm^{-3})	DIG scale height (pc)	Hα scale height (pc)
Fiducial	0.0032	0	0.1	Yes	7.81	0.0087 ± 0.0003	766 ± 21	291 ± 6
Equilbrium	0.0032	0	0.1	No	7.81	0.0064 ± 0.0019	343 ± 34	197 ± 24
HighSFR	0.01	0	0.1	Yes	7.81	0.0264 ± 0.0020	442 ± 17	227 ± 7
LowSFR	0.0005	0	0.1	Yes	7.81	0.00020 ± 0.00001	2913 ± 363	782 ± 37
HOLMESLOW	0.0032	5×10^{45}	0.1	Yes	7.81	0.0203 ± 0.0006	967 ± 25	361 ± 5
HOLMESMID	0.0032	1×10^{46}	0.1	Yes	7.81	0.0440 ± 0.0014	633 ± 11	293 ± 4
DIM	0.0032	0	0.02	Yes	7.81	0.0063 ± 0.0002	1183 ± 29	422 ± 7
BRIGHT	0.0032	0	0.5	Yes	7.81	0.0330 ± 0.0025	517 ± 16	226 ± 6
NOPHOTONS	0.0032	0	0.0	Yes	7.81	0.0041 ± 0.0001	1850 ± 81	569 ± 15

3 RESULTS

3.1 Summary of models

Table 1 displays the input parameters, and resulting fits for the vertical structure of the DIG in our simulations. All simulations were run on the previously described Cartesian grid with dimensions of 1 kpc × 1 kpc × 6 kpc.

The DIG parameters are retrieved by taking a median warm ionized hydrogen density at each height throughout the time period of 150–300 Myr, and fitting to a simple exponential function. Warm gas is selected as having $300K < T < 15000K$. The mid-plane regions ($|z| < 200$ pc) are not included in the fit and neither are regions close to the upper and lower boundaries ($|z| > 2$ kpc). The uncertainties are determined from the covariance matrix of each fit, with the standard deviation of density/Hα at each height being used as the input uncertainties.

- В табл. 1 — входные (начальные) параметры и итоговые параметры фитса для экспоненциальной вертикальной шкалы (в красной рамке)

Fiducial model / Опорная модель

Структура единичного моментального снимка, вплоть до высот ±2 кпк на 350 Myr

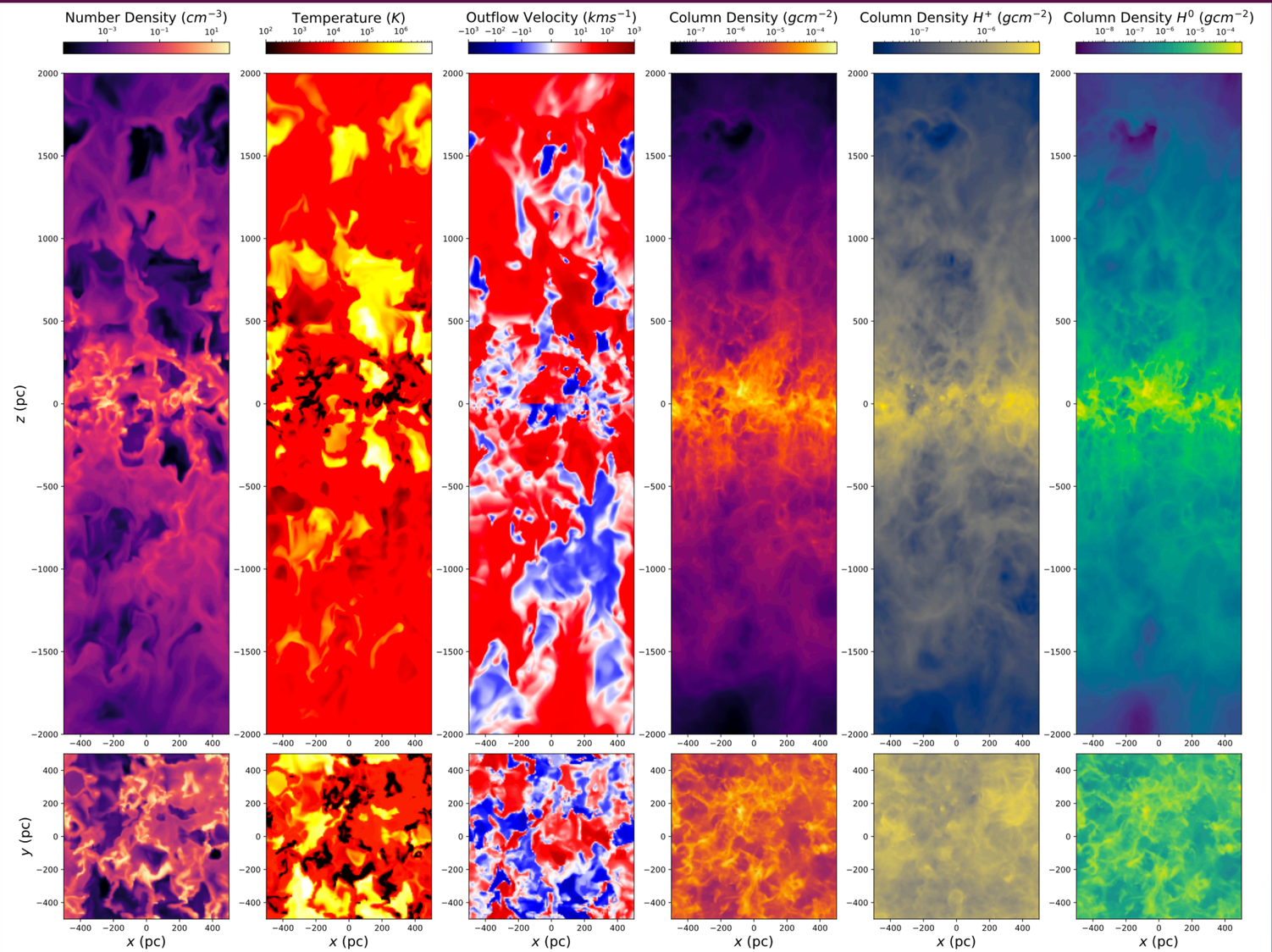

Figure 3. A visualization of a snapshot from the fiducial model at a time of 350 Myr. First column shows a slice of total hydrogen number density through the centre of the grid, upper panel is a vertical slice and lower panel shows the density in the mid-plane. Second column shows temperature slices. Third column shows outflow velocity slices, $d|z|/dt$. Fourth column shows total projected hydrogen column density along the y (upper panel) and z (lower panel) axes. Columns five and six show the projected column density of neutral and ionized gas.

Fiducial model / Опорная модель

Первые 150 Myr эволюции (?) of edge on projected column density (?)

ized). The photon transport is inhibited in uniform media. Turbulent outflows or turbulence due to supernovae are crucial in the support of ionized gas at altitude. This means that the high altitude gas remains neutral until the simulations develop outflows.

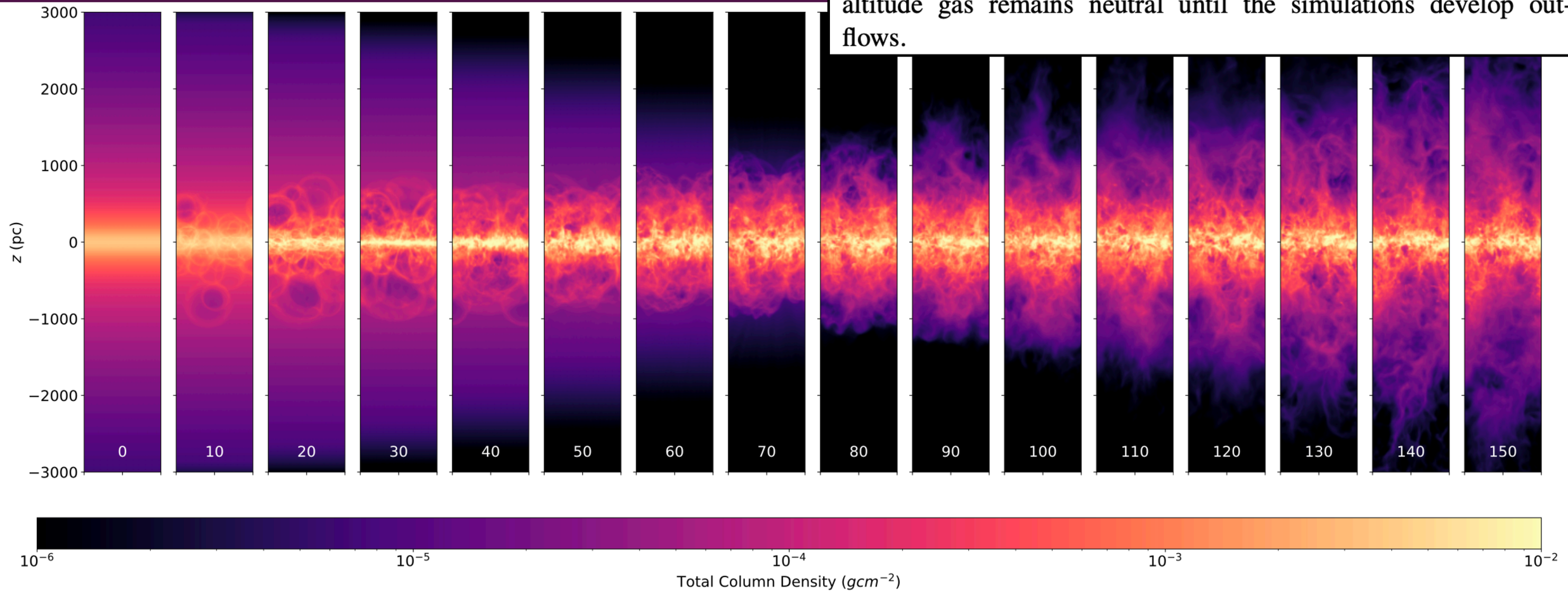

Figure 4. Evolution of edge on projected total column density for the first period of inflow and outflow in our fiducial model. White text at the bottom of each panel shows the evolution time in Myr.

Fiducial model / Опорная модель

Эволюция SFR на протяжении 500 Myr: подъем и изменчивость

Looking at the evolution of the star formation rate throughout the simulation in Fig. 5, we see the SFR increases steadily as the simulation begins in a state of inflow, increasing the mid-plane mass and hence the SFR. The SFR continues to vary throughout the simulation as the evolution goes through periods of net outflow and inflow from and into the disc. These periods of inflow and outflow are also noted in the simulations of Walch et al. (2015) and Kado-Fong et al. (2020).

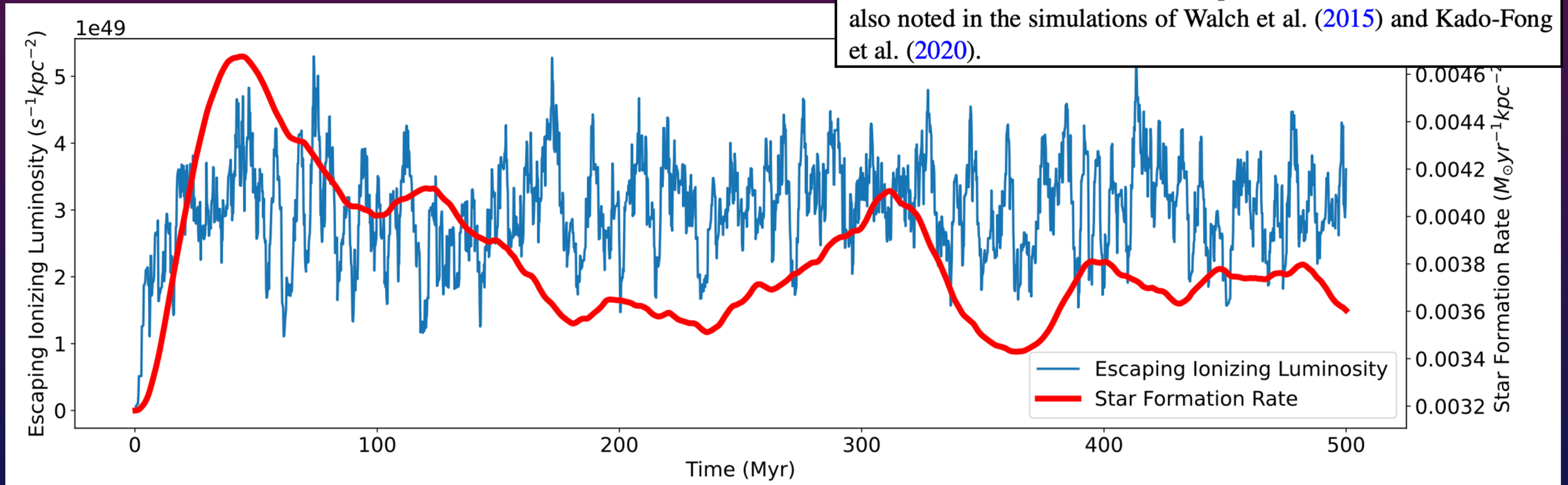

Figure 5. The evolution of total escaping luminosity within the simulation box, and SFR throughout 500 Myr of evolution. SFR is calculated at each step as a function of the amount of mass within 200 pc of the mid-plane. Smoothed luminosity has been averaged over a 10 Myr uniform filter.

Fiducial model / Опорная модель

Медианная для 150–500 Myr структура плотности нейтрального и ионизованного водорода ±1σ в зависимости от галактической высоты z и сравнение с ожидаемыми

- Нейтральный водород соответствует ожиданиям, а DIG имеет ту же шкалу высот, но меньшие плотности

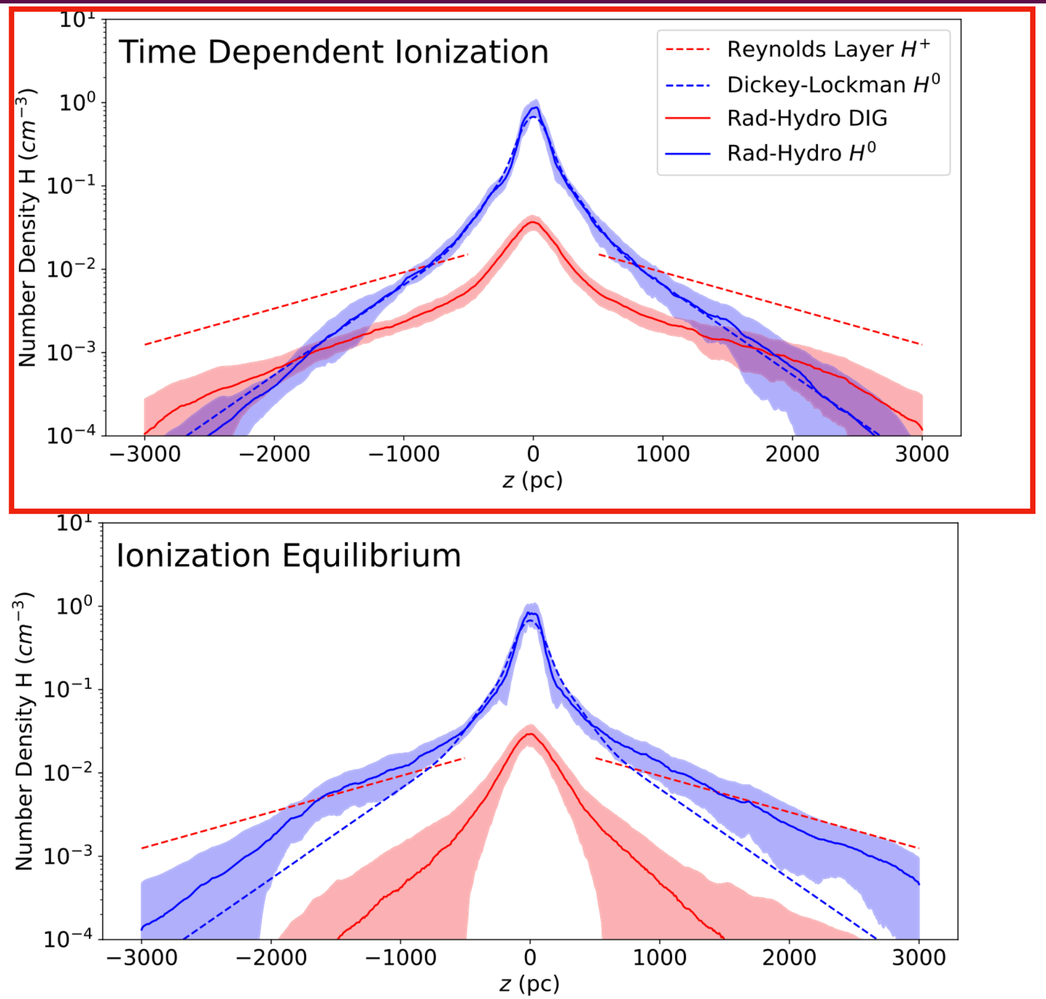

Figure 6. Vertical extent of neutral and warm ionized hydrogen both in the Milky Way and in our fiducial (time-dependent non-equilibrium ionization) and equilibrium-ionization simulations. Solid lines show the median densities throughout the simulation snapshots for times 150–500 Myr. Blue dashed lines represent the Dickey–Lockman distribution for neutral hydrogen in the Milky Way, and red dashed lines show the inferred Reynolds layer for ionized hydrogen. The red solid lines in each panel show the warm ionized structure ($T < 15\,000$ K) from our simulations, and the solid blue lines show the neutral structure. The upper panel shows results of our fiducial model (with our non-equilibrium ionization scheme), and the lower panel shows the results given the assumption of ionization equilibrium. Shaded regions cover 1σ intervals. Note that the 1σ dispersion of the warm ionized gas is much smaller in our time-dependent ionization simulations. Compared to simulations adopting ionization equilibrium, our time-dependent ionization and recombination scheme yields persistent widespread warm ionized gas at higher densities and with less temporal variability. See also Fig. 9 for images demonstrating the difference in the simulations.

Fiducial model / Опорная модель

Объемный фактор заполнения горячей ионизованной среды (T > 15000 K), теплой ионизованной среды (T < 15000 K), и полной нейтральной среды (теплой + холодной)

- Mid-plane volume filling factor of the DIG is~ 30%, increasing to~ 80% at the top of our simulation box.
- The mid-plane volume filling factor of WIM/DIG in our fiducial model is close to the observational estimate from Tielens (2005) and the SILCC simulations from Rathjen et al. (2021). Similar to the SILCC simulations our model underestimates the mid-plane mass fraction of the DIG compared to observational estimates

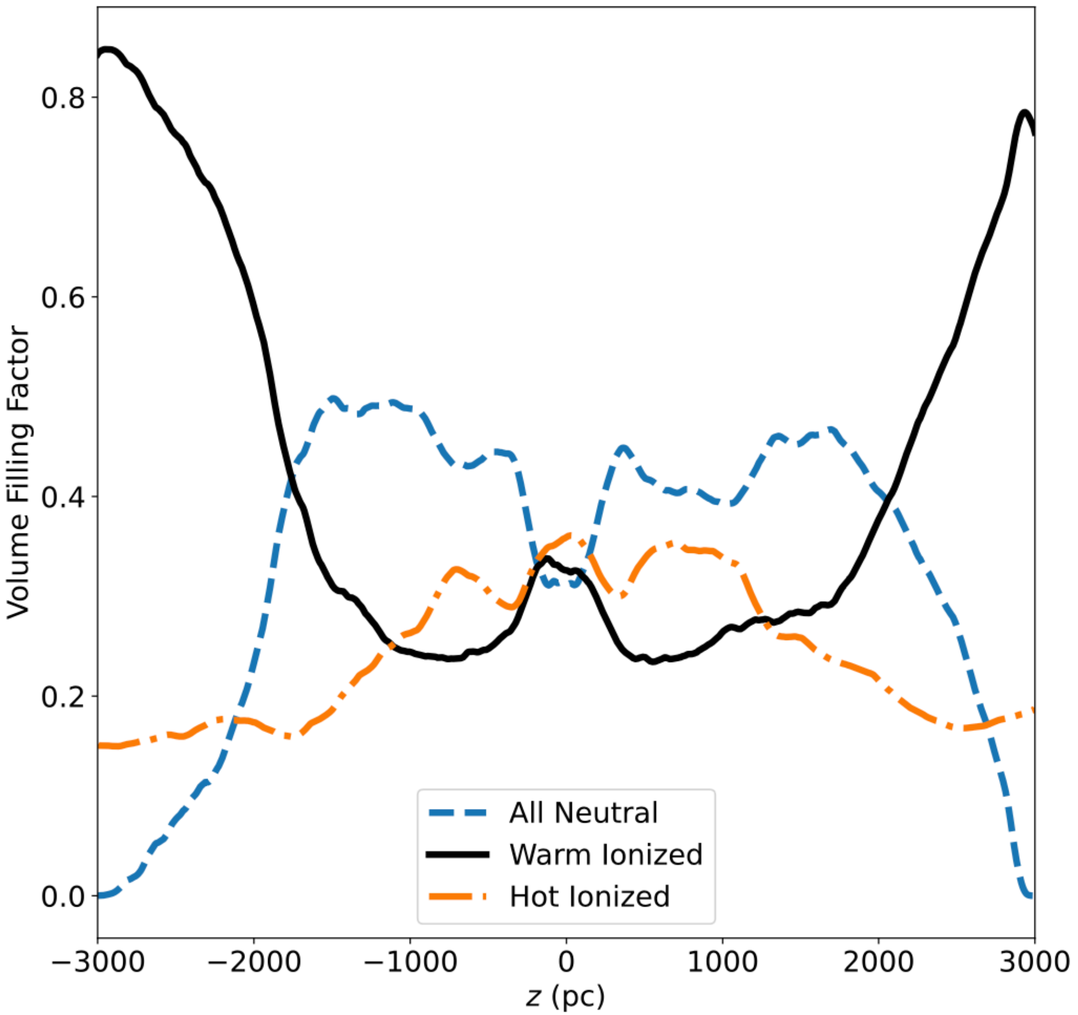

Figure 7. Volume filling factors of the hot ionized medium ($T > 15000$ K), warm ionized medium ($T < 15000$ K), and neutral gas as a function of height in the fiducial model. The lines show mean values for the volume filling factors in our fiducial simulation for all snapshots from 150 to 500 Myr.

Недопустимость ионизационного равновесия

Изменение шкалы высот DIG со временем для различных режимов симуляций

following runs, fiducial, equilibrium, and HOLMESLOW. Again it can be seen that the equilibrium run produces much smaller and more variable scale heights than the run utilizing the full non-equilibrium calculation. The DIG scale height is seen to increase and decrease

Also displayed in Fig. 8 is the time-evolution of the DIG scale height in the HOLMESLOW simulation. While both the fiducial and HOLMESLOW run oscillate between states of high and low DIG scale height, the simulation including a dim population of HOLMES sources is seen to support a DIG layer with a higher scale height for longer, and one which recovers faster after a period of inflow. The

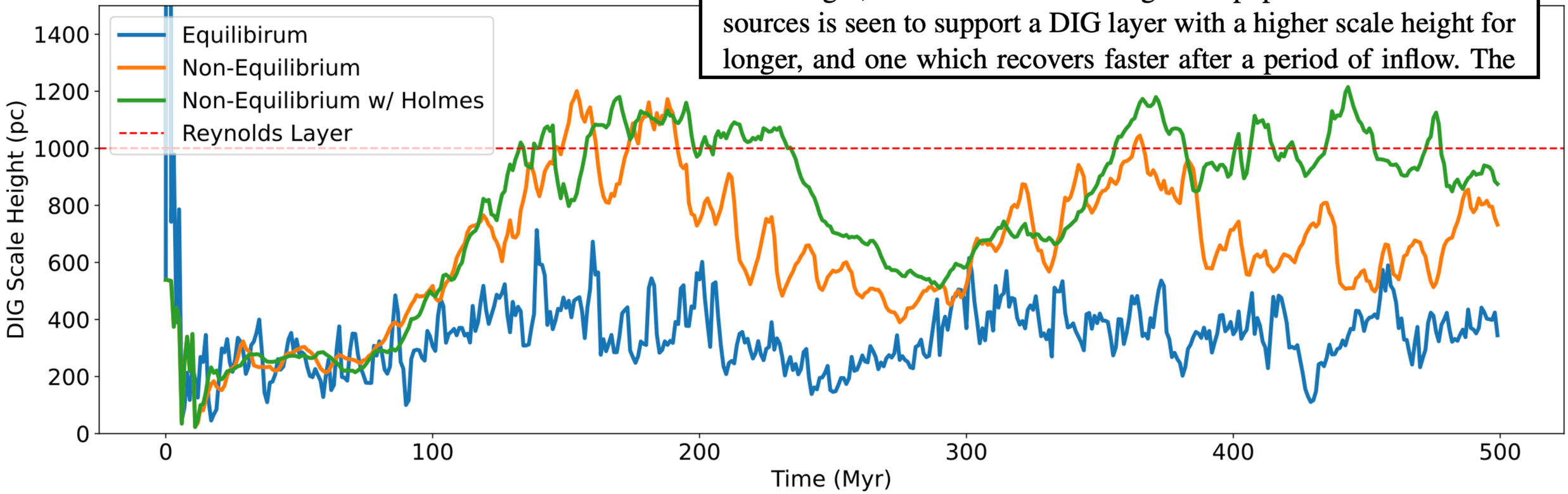

Figure 8. Time evolution of scale height of DIG layer in simulations fiducial, equilibrium, and HOLMESLOW. Scale heights are derived from fitting to decreasing exponential. Heights of $|z| < 500$pc and $|z| > 2000$pc are not included in the fit. DIG is defined as ionized gas with $T < 15000$K.

Недопустимость ионизационного равновесия

Сравнение эволюции с учетом неравновесности и без учета

the simulation is similar in general structure. However, the ionized fractions above heights of 1 kpc are vastly different in the equilibrium run, and the ionized hydrogen mass at height is very time variable.

volume of gas. The stochasticity in the escaping ionizing luminosity combined with these projection effects without a limiter on rate of change of ionization state gives a flickering effect to the ionized gas structure.

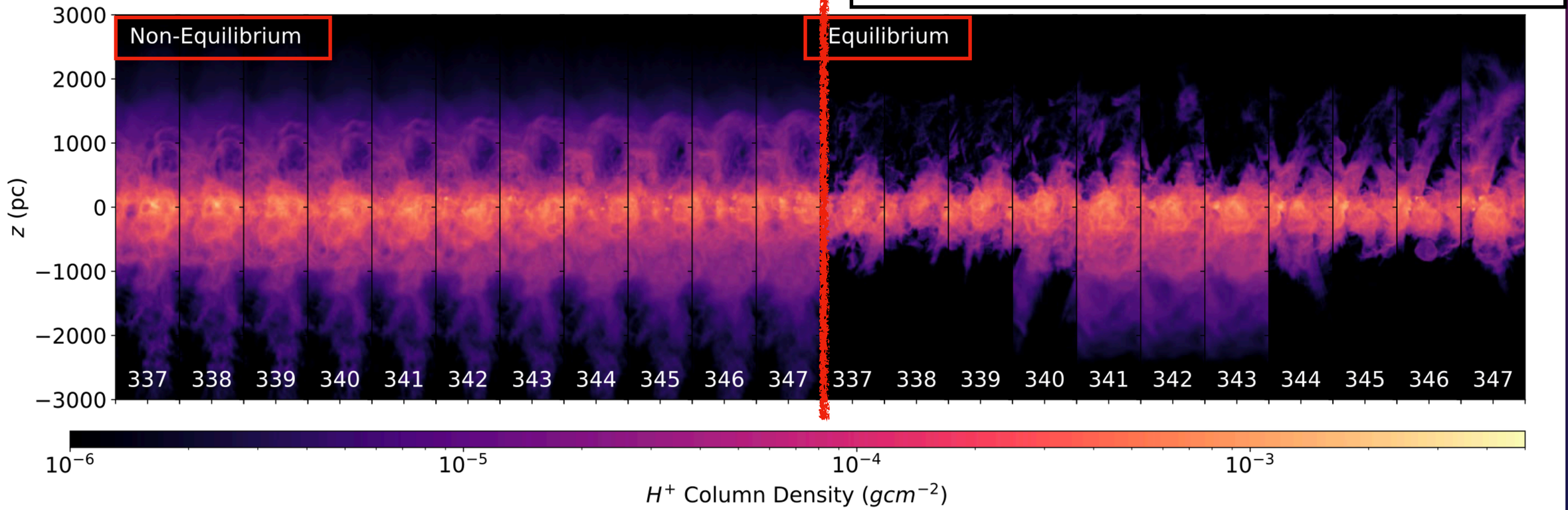

Figure 9. An illustration of the 'flickering' effect in the ionization equilibrium simulation. Panels show the edge-on column density of ionized hydrogen at various times between 337 and 347 Myr. The leftmost 11 panels (labelled 'Non-Equilibrium') show the results of our fiducial (time dependent non-equilibrium ionization) simulation. The rightmost 11 panels (labelled 'Equilibrium') show the ionization equilibrium simulation. White text at the bottom of each panel shows the simulation time in Myr. Note the extent and stability of the ionized gas in the non-equilibrium (time dependent) ionization simulation. The flickering effect in the ionization equilibrium simulation is evident between 341 and 343 Myr where the ionized gas is briefly much more extended.

Влияние HOLMES

Fig. 10 displays the results of the three simulations including hot evolved low mass sources of differing ionizing luminosities, alongside the fiducial run of the same SFR. From Fig. 5, we see

Compared to the Dickey–Lockman distribution, the fiducial run has more neutral gas at large altitudes, and in these regions produces less ionized hydrogen than the Milky Way's Reynolds layer. Fig. 10 demonstrates that more DIG is produced with increasing ionizing luminosity from the low mass stars. The simulation with a total ionizing luminosity from low mass stars of $5 \times 10^{48} s^{-1} kpc^{-2}$ (approximately 2.0 per cent of total available) most closely matches the Reynolds layer.

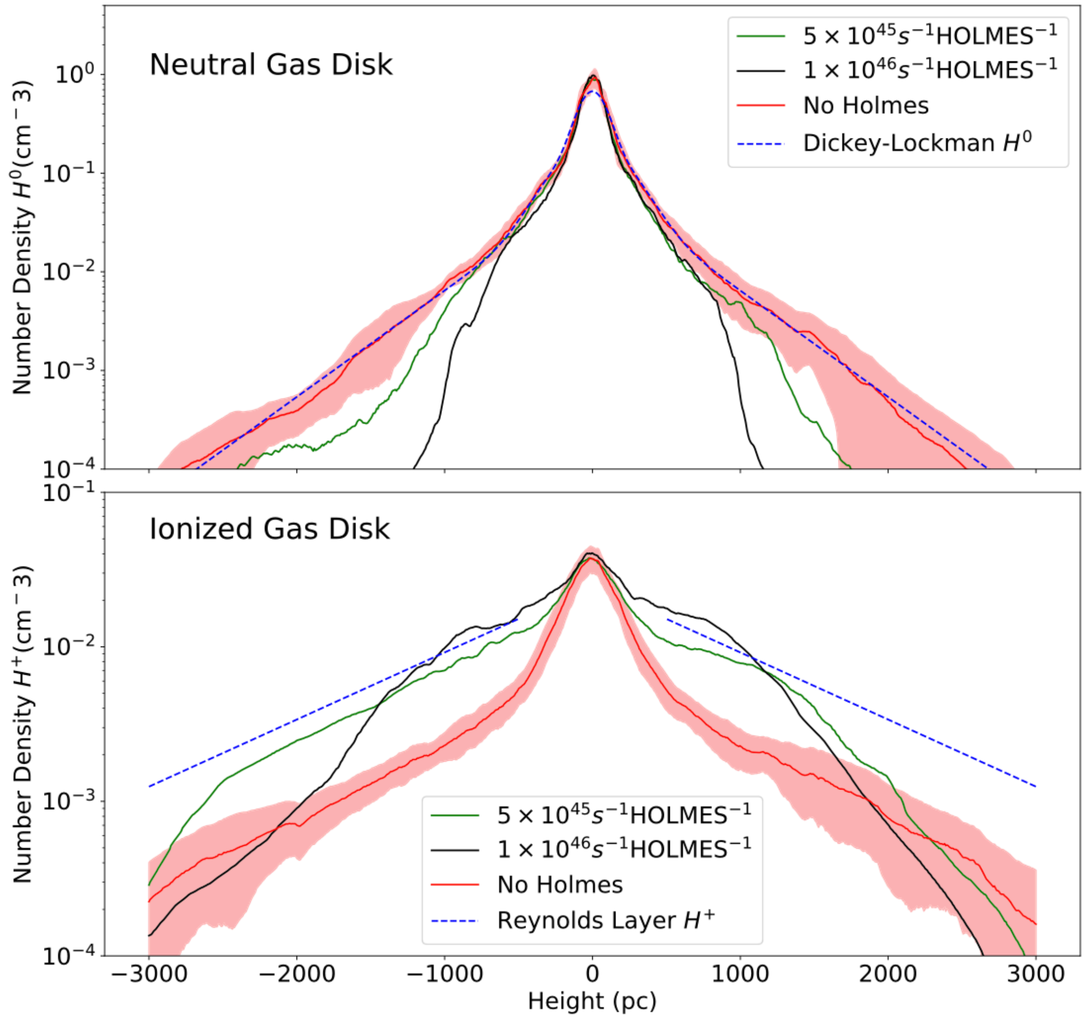

Figure 10. Vertical extent of neutral and ionized hydrogen both in the Milky Way and in our HOLMES simulations. Solid lines show the median densities throughout the simulation snapshots. Lower panel shows ionized hydrogen and upper panel is neutral. Dashed blue lines show the inferred neutral and ionized density structure for the Milky Way, solid lines represent simulations with different HOLMES luminosities. Lines are median value for each height throughout all snapshots from 150 to 300 Myr. Red fill on each panel shows 1σ variation around the control run with no HOLMES.

Влияние HOLMES

structure is very close to expected densities. Fig. 11 shows the median structure from 150 to 220 Myr in the HOLMESLOW simulation which is very close Milky Way structures.

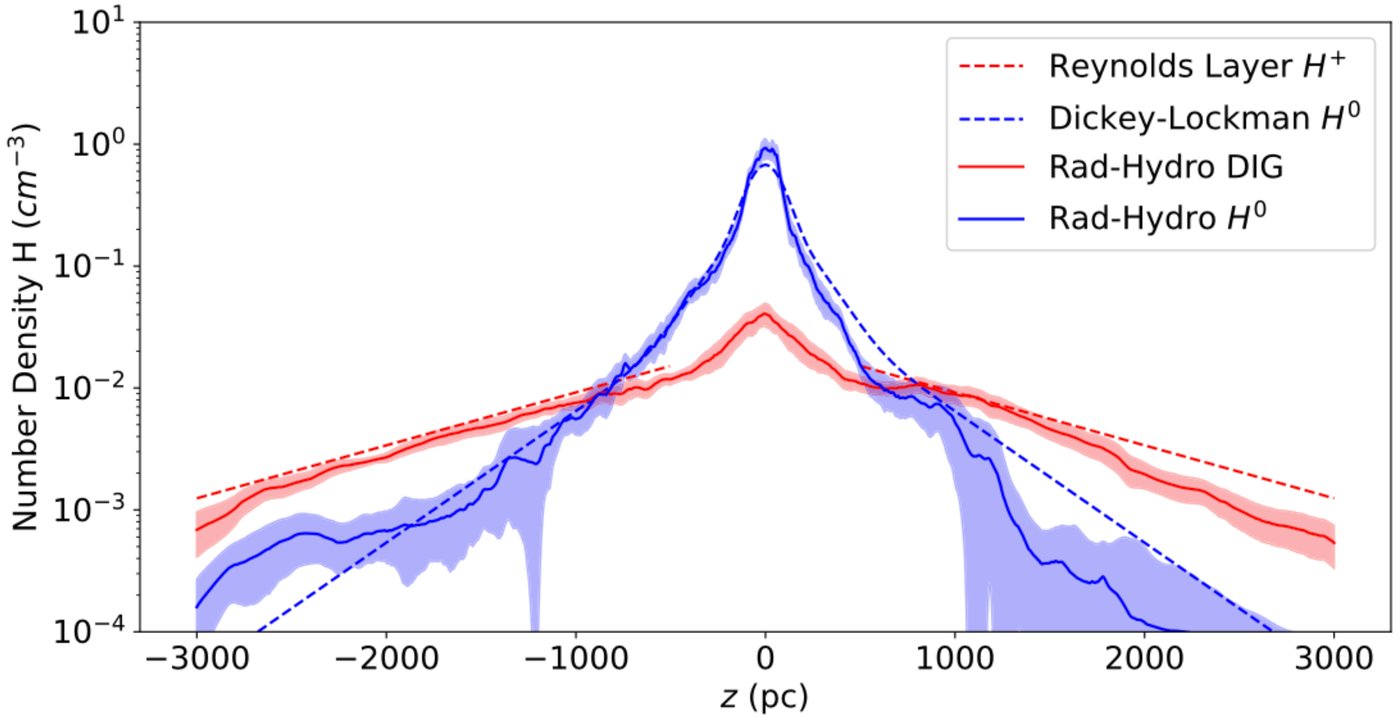

Figure 11. Vertical extent of neutral and warm ionized hydrogen both in the Milky Way and in our HOLMESLOW simulation averaged from 150 to 220 Myr. Lines are the same as Fig. 6.

Влияние SFR

Our fiducial model was initialized such that the SFR within the box was close to the mean Milky Way value ($3.2 \times 10^{-3}\,M_\odot\,yr^{-1}\,kpc^{-2}$), and then allowed to change in proportion to the gas mass below a height of 200 pc as $M_{gas}^{1.4}$. This initial SFR sets the normalization of the Kennicutt–Schmidt relation (equation 10). We note from the work of Elia et al. (2022) that the SFR surface density varies throughout the Milky Way by one to two orders of magnitude. We therefore ran two further simulations representing a low and high star formation rate of $5 \times 10^{-4}\,M_\odot\,yr^{-1}\,kpc^{-2}$ and $1 \times 10^{-2}\,M_\odot\,yr^{-1}\,kpc^{-2}$.

Влияние SFR

Низкий SFR

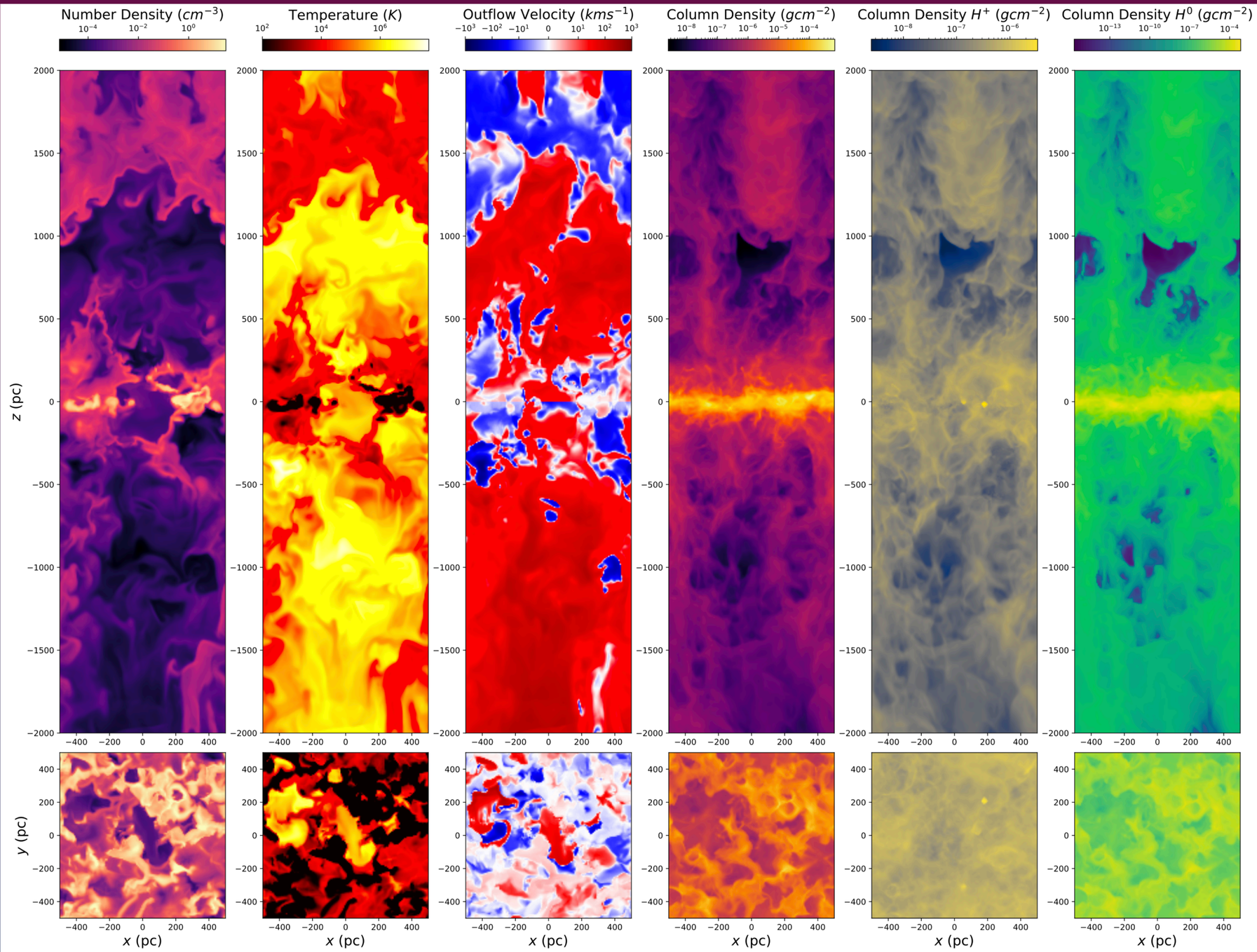

Figure 12. A visualization of a snapshot from the low SFR model at a time of 350 Myr. Columns are the same as Fig. 3.

Влияние SFR

Низкий SFR

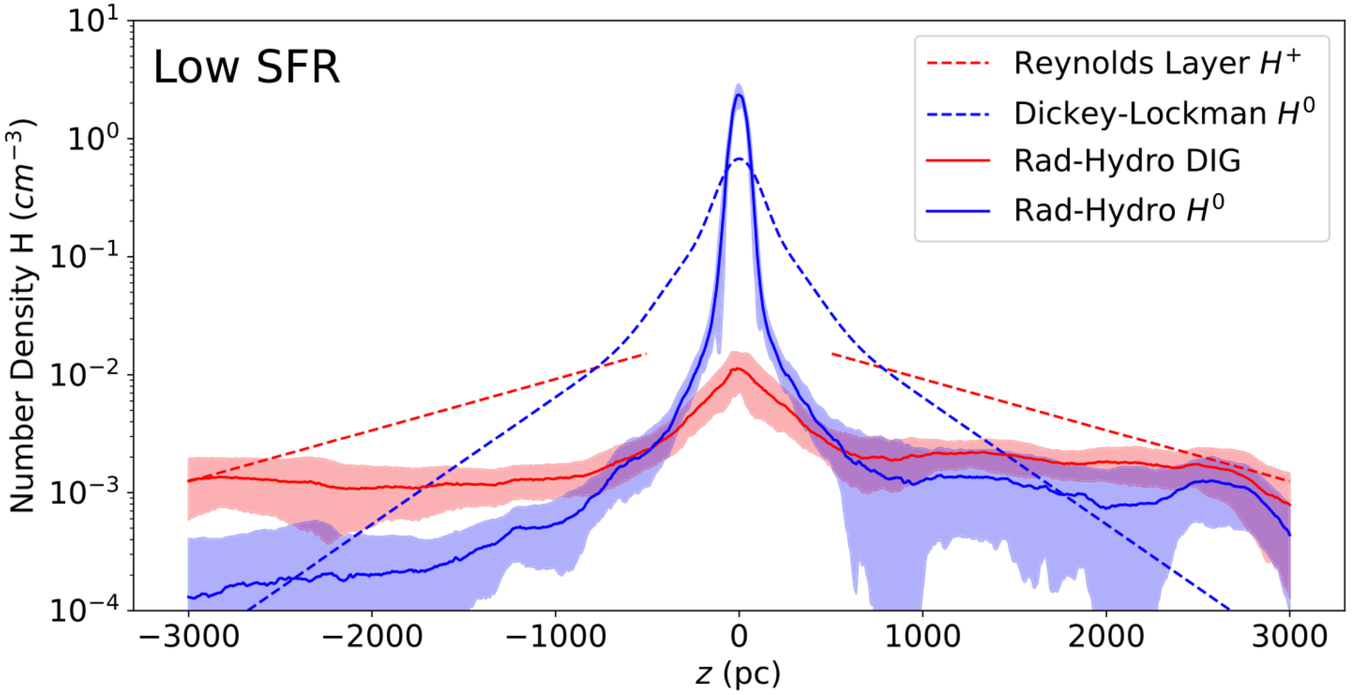

Figure 13. Vertical extent of neutral and ionized hydrogen both in the Milky Way and in our low SFR simulation. Lines and shaded regions are the same as in Fig. 6. Results are median value for all snapshots from 150 to 400 Myr. Note that the neutral material is much more sharply confined to the mid-plane, and there is less material supported at height.

Влияние SFR

Высокий SFR

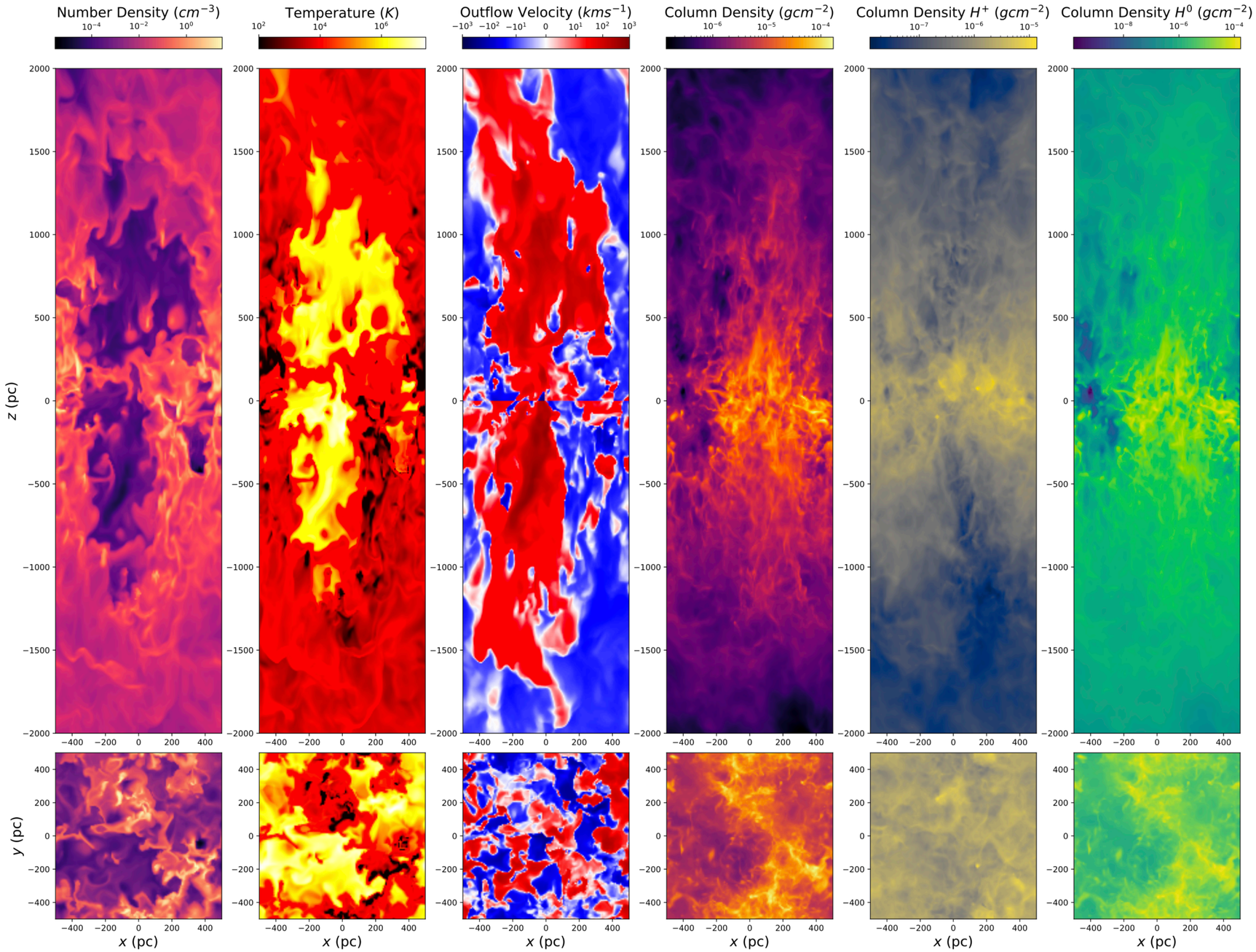

Figure 14. A visualization of a snapshot from the high SFR model at a time of 350 Myr. Columns are the same as Fig. 3. Note that the disc is almost completely disrupted and there is much more material at high altitudes.

Влияние SFR

Высокий SFR

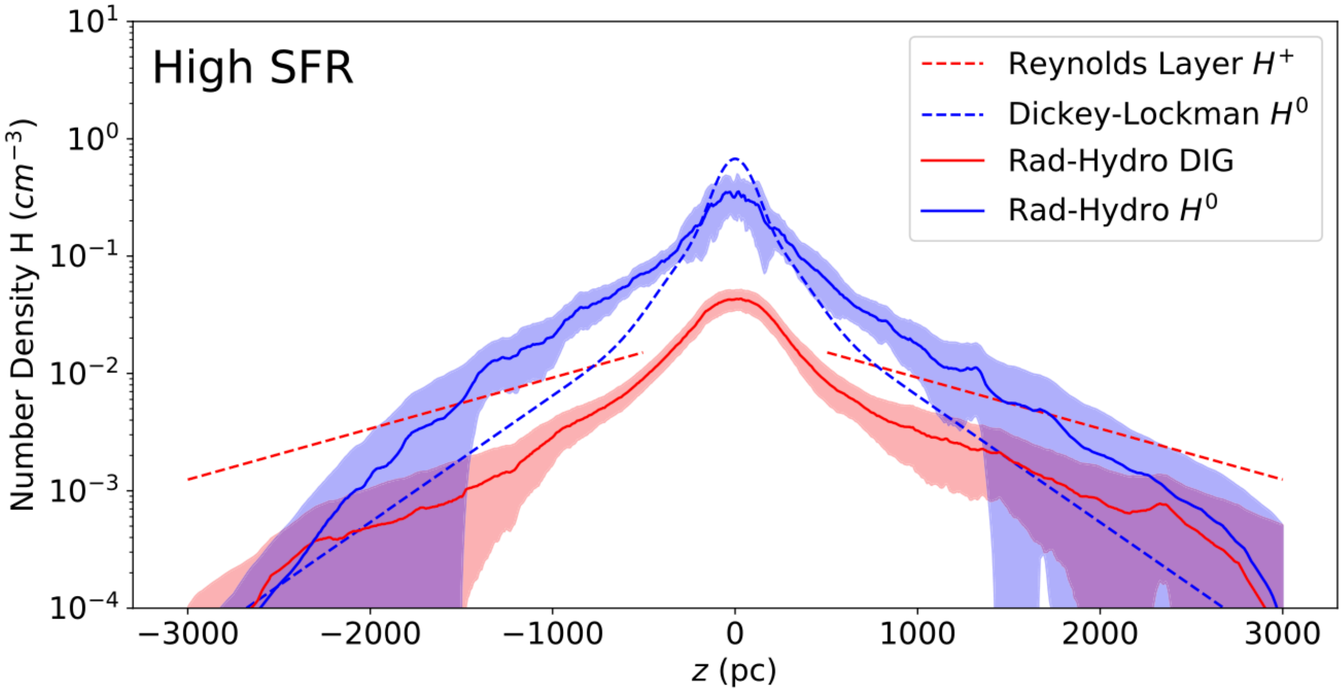

Figure 15. Vertical extent of neutral and ionized hydrogen both in the Milky Way and in our high SFR simulation. Lines and shaded regions are the same as in Fig. 6. Results are median value for all snapshots from 150 to 400 Myr. Note that the neutral disc has been destroyed near the mid-plane, and there is an increased amount of material at heights of 500–2 kpc.

Выводы - 1

- Исследовали влияние различных параметров: ионизационного равновесия, SFR, HOLMES, степени утечки ионизирующий фотонов из молекулярных облаков, — на состояние газа на различных высотах в сравнении с MW

- Подтвердили отсутствие DIG на больших высотах в предположении **ионизационного равновесия**, как и в симуляциях Kado-Fong et al. (2020):

The impact of a population of hot low mass evolved stars on the ionization state of the high altitude gas was investigated, as well as a study into the effect of varying star formation rates. The effect of varying SFR on the vertically resolved ISM is primarily seen in the shape of the neutral disc. Low values of SFR inhibit outflows and result in a sharp and dense disc, whereas high values tend to destroy the disc and power strong outflows to high altitudes. This is in broad agreement with other tall-box simulations of the ISM. Rathjen et al. (2023) investigated different surface densities in MHD simulations with self-consistent sink particle star formation, and found that powerful bursts of star formation would completely disrupt the disc, but low surface densities do not power outflows to support DIG-like structures. We similarly see close agreement to the simulations of Kado-Fong et al. (2020) in our control simulations enforcing ionization equilibrium, whereby material is supported at height by the supernova feedback, but not held at a high enough ionization state to recreate the observed Reynolds layer.

Kado-Fong et al. (2020) performed MHD simulations of the ISM including the effects of supernovae, using a self-consistent star formation algorithm based on sink particle formation and the assumption of ionization equilibrium. The vertically resolved neutral structure reproduced that of the Milky Way, but the DIG layer in their simulations was highly variable in time and only occasionally reached the kpc scale heights inferred from observations. The assumption of ionization equilibrium and the absence of accreting gas from the intergalactic medium were suggested as possible explanations for the low density of the DIG in their simulations. Another source of ionization of the DIG in addi-

In summary, we agree with the findings of Kado-Fong et al. (2020) that when photoionization equilibrium is assumed the resulting DIG is highly variable and not as extended as in the Milky Way. The inclusion of non-equilibrium ionization in our simulations maintains the DIG at high altitudes resulting in neutral and ionized density profiles similar to those inferred for the Milky Way.

Выводы - 2

The most important code development relating to the simulation of low density diffuse ionized gas is the inclusion of a time-dependent ionization state calculator to follow the ionization and recombination of the DIG. If ionization equilibrium is assumed, a Milky Way-like DIG layer is rarely formed. At DIG densities the recombination time-scales can exceed tens of millions of years. We find that the calculation of the ionization state in a time-dependent manner is crucial for the study of ionized gas at DIG densities.

- Совершенствование кода симуляции DIG благодаря включению рассмотрения ионизационного состояния DIG соответственно развитию модели во времени, а не на этапе пост-обработки — является ключевым для изучения ионизованного газа при плотностях, соответствующих DIG, иначе слой DIG почти не будет формироваться

Выводы - 3

We find that a star formation rate of 0.0032 $M_{\odot}yr^{-1}kpc^{-2}$ matches the Dickey–Lockman distribution of neutral gas. The required ionizing luminosity from hot evolved low mass stars to reproduce both the neutral and ionized densities at height is harder to constrain due to the stochasticity inherent to the simulations, and the dependence of this on other parameters. However, we find that a value of 5×10^{48} $s^{-1}kpc^{-2}$ produces close to expected density of neutral and ionized material at high altitudes for many snapshots. This represents 2.0 per cent of the total available ionizing luminosity.

- $\Phi_{HOLMES} = 8.4 \cdot 10^4 photons/s/cm^2$ - const for all the models

- SFR 0.0032 Ms/yr/kpc^2 достаточно для воспроизведения распределения нейтрального газа Дики-Локмана
- Ионизирующее излучение от HOLMES порядка 5x10^{48} фотонов/s/kpc^2 достаточно для воспроизведения нейтрального и ионизованного газа наблюдаемых плотностей на больших высотах, что составляет 2% от полного ионизирующего излучения (в соответствующих фотоионизационных моделях 3MdB заложено значение, в принципе, близкое по порядку: 8.4x10^4 фотонов/s/kpc^2 = 8.0x10^{47} фотонов/s/kpc^2)
- В результате симуляций вертикальное распределение нейтрального и ионизованного газа получается близким к наблюдаемому в MW

- Объемный фактор заполнения DIG увеличивается с галактической высотой, что может привести в согласие расхождения между измерениями шкалы высот по Ha и по пульсарам

It is seen in all of our simulations that the volume filling factor of DIG rises with height above the mid-plane up to our simulation box ceiling at 3 kpc. This result can be used to reconcile tensions between H α and pulsar dispersion measurements of DIG scale height, with the H α derived electron scale height often presenting as less than 75 per cent of the true value.

3.3.2 Pulsar dispersion versus H α scale height

Two commonly used observational techniques to measure DIG scale height are pulsar dispersion measures, and the spatial distribution of H α emission. The former is proportional to the total integrated electron density whereas the latter is proportional to integrated electron density squared. H α scale heights are hence often simply doubled to infer a DIG/free electron scale height following an assumption of a constant volume filling factor (Hill et al. 2014; Krishnarao et al. 2017). It can be seen in Table 1, however, that in all simulations the H α scale height is less than half the DIG scale height. This can be explained by a rising DIG volume filling factor with height, which is evident in the fiducial model in Fig. 7. Note we are using DIG scale height and free electron scale height interchangeably here, due to the negligible mass fraction of the HIM as seen in both observations and simulations in Table 2. From the pulsar dispersion measure results of Ocker et al. (2020), the local free electron scale height has been measured as $1.57^{+0.15}_{-0.14}$ kpc, with a mid-plane density of 0.015 cm^{-3}. Using our simulation HOLMESLOW as the closest DIG layer in vertical structure to these observed values, we find the H α derived electron scale height of 722 pc to be approximately 75 per cent of the true DIG scale height in that simulation.

Haffner 2009

Two fundamental parameters of ionized gas along any line of sight, s, are the dispersion measures (DM $\equiv \int n_e\, ds$), derived from pulsar observations, and the emission measure (EM $\equiv \int n_e n_{H^+}\, ds \approx \int n_e^2\, ds$), derived from the intensity of the hydrogen Balmer-alpha (Hα) recombination line or from the amount of free-free (Bremsstrahlung) emission or absorption. Comparison of these measurements along common lines of sight indicate that the H^+ is clumped into regions having an average electron density, $n_e = 0.03$–0.08 cm^{-3}, and filling a fraction, $f \approx 0.4$–0.2, of the volume within a 2000–3000 pc thick layer about the Galactic midplane (Hill *et al.*, 2008; Reynolds, 1991b). Data also suggest that the filling fraction increases from $f \sim 0.1$ at the midplane to $f > 0.3$–0.4 at $|z| = 1000$ pc (Berkhuijsen *et al.*, 2006; Gaensler *et al.*, 2008; Kulkarni and Heiles, 1987; Reynolds, 1991b). The large, 1000–1800 pc scale height, significantly larger than that of the neutral hydrogen layer, has been deduced from both pulsar observations (Gaensler *et al.*, 2008; Reynolds, 1989) and from the rate of decrease in the Hα intensity with increasing Galactic latitude for the gas associated with the Perseus spiral arm (e.g., Haffner *et al.*, 1999). The WIM accounts for 90% or more of the ionized hydrogen within the interstellar medium, and along lines of sight at high Galactic latitude (i.e., away from the Galactic midplane), the column density of the H^+ is approximately 1/3 that of the neutral hydrogen (Reynolds, 1991a).

Haffner 2010

Shortly following their work, the discovery of pulsars (Hewish et al. 1968) afforded a direct measure of the free electron column along lines of sight since their dispersion measure (DM $\equiv \int n_e\, dl$) causes a time delay in pulse arrival as a function of frequency. Significant dispersion measures are seen toward pulsars—especially those above the plane—that have no obvious ionized region along the line of sight.

Сравнение с предыдущей статьей по теме

Учет/неучет двойственности звезд => необходимость HOLMES

The nature of diffuse ionised gas in star-forming galaxies

William McClymont,[1,2]★ Sandro Tacchella,[1,2] Aaron Smith,[3] Rahul Kannan,[4] Roberto Maiolino,[1,2] Francesco Belfiore,[5] Lars Hernquist,[6] Hui Li[7] and Mark Vogelsberger[8]

[1]*Kavli Institute for Cosmology, University of Cambridge, Madingley Road, Cambridge CB3 0HA, UK*
[2]*Cavendish Laboratory, University of Cambridge, 19 JJ Thomson Avenue, Cambridge CB3 0HE, UK*
[3]*Department of Physics, The University of Texas at Dallas, Richardson, Texas 75080, USA*
[4]*Department of Physics and Astronomy, York University, 4700 Keele Street, Toronto, ON M3J 1P3, Canada*
[5]*INAF — Arcetri Astrophysical Observatory, Largo E. Fermi 5, I-50125, Florence, Italy*
[6]*Center for Astrophysics | Harvard & Smithsonian, 60 Garden Street, Cambridge, MA 02138, USA*
[7]*Department of Astronomy, Tsinghua University, Beijing 100084, People's Republic of China*
[8]*Department of Physics and MIT Kavli Institute for Astrophysics and Space Research, 77 Massachusetts Avenue, Cambridge, MA 02139, USA*

Accepted XXX. Received YYY; in original form ZZZ

ABSTRACT

We present an analysis of the diffuse ionised gas (DIG) in a high-resolution simulation of an isolated Milky Way-like galaxy, incorporating on-the-fly radiative transfer and non-equilibrium thermochemistry. We utilise the Monte-Carlo radiative transfer code COLT to self-consistently obtain ionisation states and line emission in post-processing. We find a clear bimodal distribution in the electron densities of ionised gas (n_e), allowing us to define a threshold of $n_e = 10\,cm^{-3}$ to differentiate DIG from H II regions. The DIG is primarily ionised by stars aged 5 – 25 Myr, which become exposed directly to low-density gas after H II regions have been cleared. Leakage from recently formed stars (< 5 Myr) is only moderately important for DIG ionisation. We forward model local observations and validate our simulated DIG against observed line ratios in [S II]/Hα, [N II]/Hα, [O I]/Hα, and [O III]/Hβ against $\Sigma_{H\alpha}$. The mock observations not only reproduce observed correlations, but also demonstrate that such trends are related to an increasing temperature and hardening ionising radiation field with decreasing n_e. The hardening of radiation within the DIG is caused by the gradual transition of the dominant ionising source with decreasing n_e from 0 Myr to 25 Myr stars, which have progressively harder intrinsic ionising spectra primarily due to the extended Wolf-Rayet phase caused by binary interactions. Consequently, the DIG line ratio trends can be attributed to ongoing star formation, rather than secondary ionisation sources, and therefore present a potent test for stellar feedback and stellar population models.

Key words: radiative transfer – galaxies: ISM – ISM: structure – ISM: lines and bands – HII regions – galaxies: stellar content